Review

Solar Desalination Driven by Organic Rankine Cycles (Orc) and Supercritical CO_2 Power Cycles: An Update

Agustín M. Delgado-Torres [1,*] and Lourdes García-Rodríguez [2]

[1] Departamento de Ingeniería Industrial, Escuela Superior de Ingeniería y Tecnología (ESIT), Universidad de La Laguna (ULL), 38200 La Laguna, Spain

[2] Departamento de Ingeniería Energética, Escuela Técnica Superior de Ingeniería (ETSI), Universidad de Sevilla, 41092 Sevilla, Spain; mgarcia17@us.es

[*] Correspondence: amdelga@ull.es; Tel.: +34-922-84-60-45

Abstract: In the field of desalination powered by renewable energies, the use of solar power cycles exhibits some favorable characteristics, such as the possibility of implementing thermal energy storage systems or a multi-generation scheme (e.g., electricity, water, cooling, hydrogen). This article presents a review of the latest design proposals in which two power cycles of great potential are considered: the organic Rankine cycle and the supercritical CO_2 power cycle, the latter of growing interest in recent years. The designs found in the literature are grouped into three main types of systems. In the case of solar ORC-based systems, the option of reverse osmosis as a desalination technology is considered in medium-temperature solar systems with storage but also with low-temperature using solar ponds. In the first case, it is also common to incorporate single-effect absorption systems for cooling production. The use of thermal desalination processes is also found in many proposals based on solar ORC. In this case, the usual configuration implies the cycle's cooling by the own desalination process. This option is also common in systems based on the supercritical CO_2 power cycle where MED technology is usually selected. Designs proposals are reviewed and assessed to point out design recommendations.

Keywords: solar ORC desalination; solar supercritical CO_2; solar desalination; solar reverse osmosis

1. Introduction

The need to change the global energy model and the increase in drinking water demand in important areas of the planet make desalination powered by renewable energies (REs) part of the solution to the future challenge of the energy–water nexus. According to International Energy Agency (IEA) data, almost 81% of the world's energy supply had its origin in fossil fuels (coal, natural gas and oil) in 2019 [1]. If we focus on electrical energy, the percentage was 63% in the same year. These values explain the still-growing trend of global greenhouse gas emission levels. In addition to this, there is the problem of access to water. According to World Bank data, internal renewable freshwater resources per capita have fallen by 36% and 25% between 2002 and 2017 in areas such as Sub-Saharan Africa or the MENA (Middle East and North Africa) region, respectively [2]. These reductions are largely due to population increase, which is the expected trend in the coming decades.

RE-powered desalination offers advantages and benefits compared to the fossil-fuels-driven option, such as the coincidence of renewable resource availability—mainly solar—and water scarcity. In addition, the environmental impacts associated with the energy consumption of the processes are reduced [3]. In this sense, the Life Cycle Analysis (LCA) of desalination technologies systematically indicates that the environmental impacts associated with the energy consumption of the process are mainly attributable to the operation and maintenance phase in comparison to construction and decommissioning phases [4]. Therefore, the use of renewables as the energy input to these processes results in a significant reduction of the environmental impacts of freshwater production. On average,

the global warming potential reduction is around 90% for conventional thermal desalination technologies—multi-stage flash (MSF) and multi-effect distillation (MED)—and 80% for reverse osmosis (RO) [4].

The above advantages justify the trend in scientific activity concerning RE-powered desalination shown in the bibliometric analysis of the scientific literature published on desalination between 2000 and 2020, as presented by Zapata-Sierra et al. [5]. Among other results, the clustering of publications is highlighted; the "Renewable energy desalination" cluster is the second most important of the eight clusters, defined with a weight of 26.1%, just one percentage point below the first "Reverse osmosis" cluster).

Within this frame, this work deals with solar-powered desalination by means of solar thermo-mechanic conversion through a power cycle, thus allowing the use of electricity and/or heat to drive desalination processes. The main aim of the paper is the review and assessment of recent design proposals existing in the literature to give design recommendations on such solar desalination systems.

The latest general review of RE-desalination concludes that the techno-economic optimization of some aspects is still necessary to offer stable solutions in the long term [6]. Regarding the solar thermal-powered option, the need for its application to both small and industrial scales and the importance of thermal energy storage are emphasized. The need to expand the implementation of off-grid systems is also indicated in general. In the field of solar thermal-powered desalination, it is possible to combine this resource with all existing desalination technologies (see Figure 1). Only the methods associated with the use of power cycles for the thermo-mechanical conversion of solar thermal energy are shown since this is the route explored in this article. Therefore, the use of the electricity generated and/or the heat rejected by a solar power cycle are the options reviewed instead of the direct coupling of thermal desalination processes to a solar thermal collector field. Concerning direct coupling, we refer to Buenaventura Pouyfacon and García-Rodríguez [7].
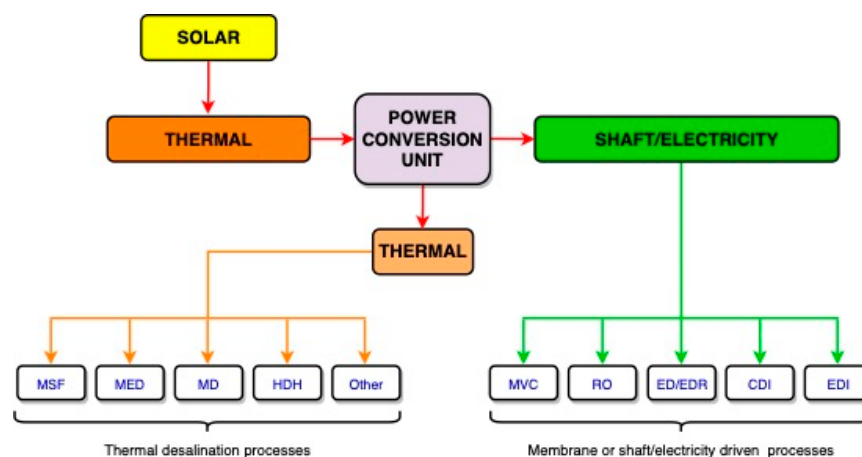

Figure 1. Possible indirect solar desalination options when a power conversion unit (power cycle) is considered as the solely final energy supply unit. MSF: multi-stage flash; MED: multi-effect distillation; MD: membrane distillation; HDH: humidification dehumidification; MVC: mechanical vapor compression; RO: reverse osmosis; ED/EDR: electrodialysis/electrodialysis reversal; CDI: capacitive deionization; EDI: electrodeionization. Adapted from [6].

The thermal processes shown in Figure 1 require a heat supply in the range of 50–120 °C [6]. Temperatures from 50 to 60 °C are only suitable for humidification dehumidification (HDH), appropriate only for small-scale use due to its relatively low energy efficiency [8]. Moreover, membrane distillation (MD) systems require 75–95 °C to achieve reasonable specific thermal consumption, up to 237 and 170 kJ/kg, respectively [7]. However, there are only small capacity units, thus limiting their application at an industrial scale. Multi-effect distillation (MED) has been superior to multi-stage flash (MSF) distillation since the end of the 20th century due to its lower main and auxiliary energy consumption

along with lower thermal consumption at the same top temperature. For the sake of comparison, the MED process achieves 230 kJ/kg of thermal energy consumption with a top temperature of 67 °C, whereas the MSF would require at least 105 °C to allow the said main energy consumption. In addition, the auxiliary energy required by the MSF process is much higher than that of MED, since the former requires brine recirculation. The industrial standard of conventional MED technology consists of a MED unit coupled to a thermal vapor compression process (MED-TVC). The MED unit is driven by the outlet flow of the TVC, which is fed by a steam extraction of the steam turbine of a Rankine cycle (motive steam) and steam generated within one of the last effects of the MED plant.

Regarding desalination processes that consume shaft power or electricity, only mechanical vapor compression (MVC) and reverse osmosis (RO) are suitable for seawater desalination applications. This is due to the significant increase in energy consumption in electrodialysis (ED), electrodialysis reversal (EDR), capacitive deionization (CDI), and electrodeionization (EDI) with salt concentration. Therefore, they do not compete with RO for salinities within the range of seawater, about 0.035 kg of sea salts per kg of saline solution.

In addition to conventional phase-change technologies, a MED unit can be coupled to a double-effect absorption heat pump (DEAHP). This technology has been developed at the Spanish research center Plataforma Solar de Almería-CIEMAT [9–11]. For a given flow and thermodynamic conditions of the external steam source, MED-DEAHP technology exhibits lower main and auxiliary energy consumptions than MED-TVC, thus resulting in higher thermodynamic efficiency of the integrated power and water production. Therefore, MED-DEAHP is superior to MED-TVC, although the former is not commercially available. Another advanced MED concept is a high-temperature MED process by using nanofiltration as seawater pretreatment. This was proposed and developed by Hassan [12–14]. Not only the concept but also the experimental assessment have been reported in the literature [15]. A representative industrial plant in which nanofiltration and distillation processes are integrated is the Sharjah plant, based on MSF distillation [16].

Analyses of integrating desalination processes within conventional solar power plants based on Rankine cycles with water as working fluid have been frequently reported in the literature, considering mostly RO, MED, and MED-TVC processes. Some exemplary papers are [17,18], among others. Regarding the integration of distillation processes, the main issue is the availability of operating models properly validated to simulate the distillation subsystem at part-load operation. Concerning MED-TVC plants, a performance model [19] has been developed to calculate the efficiency and water production of the MED-TVC distillation process as a whole within a suitable range of the external steam source. Some selected previous papers are Hanafi et al. [20], who described a thorough model of a thermocompressor for the said application, and Ameri et al. [21] and Mazini et al. [22], who presented useful models of MED-TVC plants. Additionally, the parametric analysis needed for plant design can be found in works by Kouhikamali et al. [23] and Esfahani et al. [24]. Finally, experimental data useful for validating models are provided by Temset et al. [25] and Al-Mutaz and Wazeer [26]. On the other hand, both MED and nanofiltration-MED processes can be modeled based on the aforementioned literature. Additionally, operation out of nominal conditions of a MED unit has been experimentally assessed by Fernandez-Izquierdo et al. [27].

Recent proposals of solar desalination system designs that fit the scheme of Figure 1 are presented throughout this paper. Minor innovations have been found concerning coupling conventional solar Rankine cycles and desalination. Indeed, innovative proposals rely on the organic Rankine cycle (ORC) and the supercritical CO_2 (sCO_2) cycle as power conversion units.

Medium-temperature technology of solar thermal collectors consists of systems with top operating temperatures within the range of 150–400 °C, thus requiring one-axis sun tracking to concentrate the solar irradiance on a linear focus in which the absorber tube is placed. Solar parabolic trough collectors (PTCs) and linear Fresnel concentrators correspond to medium-temperature collectors. Since conventional Rankine cycles operated with

water exhibit quite limited efficiency at relatively low temperatures, significant research activity has been focused on organic Rankine cycles (ORCs), suitable even for the lowest temperatures within the said range. Indeed, ORCs operated with low-temperature solar collectors—i.e., stationary collectors—have also been developed. The first solar ORC desalination systems date back to the late 1970s and early 1980s, all of them using reverse osmosis as the desalination technology. Due to the high specific energy consumption of the process at that time, these first experiences were developed for brackish water desalination [28–30]. A review of state-of-the-art solar thermal reverse osmosis desalination systems up to 2009 can be found in [31]. Its conclusions indicate, among other issues, that the water–electricity cogeneration option has not been sufficiently explored. Design recommendations based on the work developed up to 2012 is reported in [32], and the update of the state of the art can be found in [33]. The existing systems and proposals are classified in the latter according to the ORC configuration into single stage (referring to simple cycles), two-stage (referring to double cascade cycles), and low-temperature systems. More recently, and covering a wider scope, the evaluation of solar thermal-powered desalination technologies has been conducted by [7] to identify market opportunities for these technologies. Among the options of growing interest is reverse osmosis powered by solar ORCs, which presents the possibility of incorporating thermal energy storage systems (TES) instead of batteries. In low demand scenarios (less than 100 m^3/d), conventional distillation technologies (MED and MSF) and RO powered by solar ORCs are discarded against the photovoltaic (PV)–RO option, while in intermediate demand scenarios (100 to 25,000 m^3/d), the solar ORCs with PTCs or Fresnel is one of the technologies with market opportunities. The following sections present the most recent proposals found in the scientific literature on solar desalination systems based on ORC as the main energy conversion units. As will be seen, the approaches based on poly- or multi-generation are dominant.

Lastly, sCO$_2$ Brayton cycles have been recently developed in order to achieve much higher energy efficiency, with top temperatures technically achievable with the current technology of solar tower power plants. Heliostats concentrate the solar radiation within a focal point on the top of a tower where the solar receiver is placed. Specifically, energy efficiency around 45% corresponds to the top temperature of 550 °C with a Brayton cycle with regeneration and recompression. In the near future, 52% could be reliable with 700 °C of top temperature [34].

2. Solar ORC (Organic Rankine Cycle)-Driven Desalination Systems: An Update

2.1. Integration of Reverse Osmosis (RO) as Desalination Technology

Reverse osmosis desalination requires electricity to power the main pump to pressurize the saline water feed above the osmotic pressure of the concentrate output flow. Pressurized feedwater flow circulates in parallel with the RO membrane surface, whereas part of the solvent passes through the membrane along with a minor portion of salts, thus generating the permeate flow (product). The remaining feed stream with increased salinity becomes the concentrate flow. Since this concentrate exits at a pressure slightly below the feed pressure, energy recovery devices are needed in seawater desalination plants. Recent proposals for solar RO desalination systems with ORC units as the prime mover generally correspond to the configurations described in the following subsections, dealing with medium- and low-temperature solar systems, respectively.

2.1.1. Medium-Temperature Solar Systems

The scheme shown in Figure 2 describes the latest innovative proposals of medium-temperature solar ORC systems. As can be seen, a solar thermal plant with thermal energy storage (TES) drives a single-effect absorption refrigeration system by the heat rejected at the condenser. This scheme would therefore respond to a poly- or multi-generational system if not the entire electrical energy output of the ORC is consumed by the RO unit. Additionally, part of this thermal energy rejected preheats the feed water of the RO system. This exploitation has two advantages: (1) the use of saline water as a cooling medium

makes an additional cooling flow unnecessary; (2) the permeability of the RO membranes rises with feed water temperature, that is to say, the productivity of the plant is improved although this occurs at the expense of an increase in the salinity of the product.
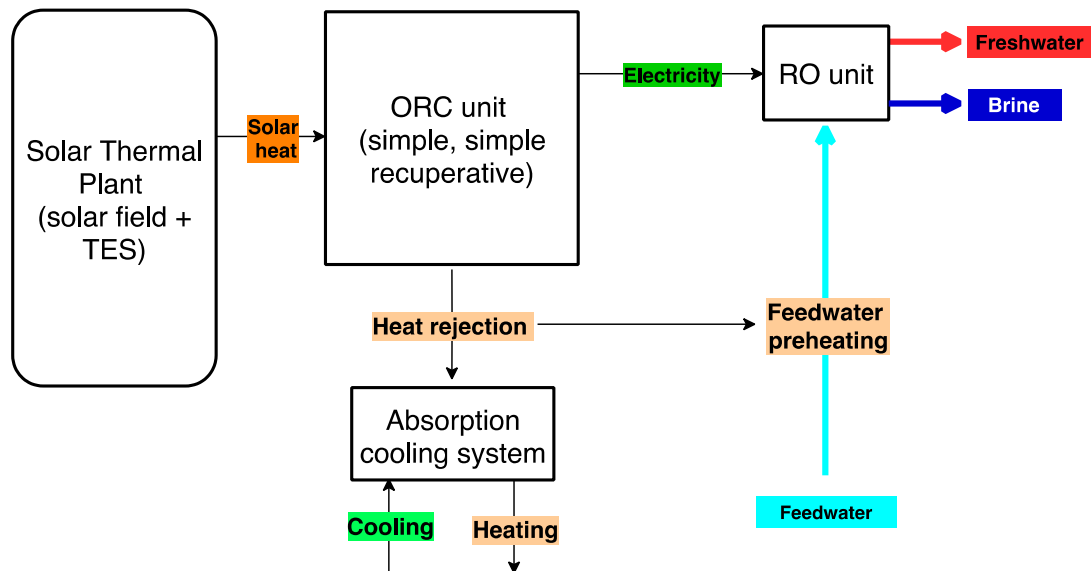

Figure 2. General scheme of a solar thermal-driven RO desalination and cooling system.

A solar poly-generation system with a recuperative ORC unit with n-octane as the working fluid for electricity production is presented in [35]. The solar system considered consists of a parabolic trough collector field operated with Therminol-66 as the heat transfer fluid (HTF) and a two-tank thermal energy storage (TES) system with commercial molten salts. Hitec XL is considered in order to take advantage of its relatively low freezing point (120 °C) and cost. A fraction of the heat transferred in the ORC's recuperator is exploited for the production of domestic hot water. Moreover, the heat rejection of the ORC is used in the generator of a single-effect absorption refrigeration cycle. The ORC's electricity output is consumed by an electrolyzer for hydrogen production and by the seawater RO unit, where a Pelton turbine is considered as the energy recovery system. The water needed in the electrolyzer is preheated by the thermal oil flow at the outlet of the ORC's solar heat exchanger. The proposed system is analyzed to produce between 200 and 500 kW electric and 450 ppm freshwater from 35,000 ppm feed water. The nominal capacity of the seawater reverse osmosis plant (SWRO) is 40 kg/s, and the absorption refrigeration system would have a cooling capacity of 500–800 kW. Both energy and exergy efficiency of the whole system is calculated, and techno-economic optimization is also performed using evolutionary algorithms.

Another configuration of parabolic trough solar collectors with TES and Therminol VP-1 as HTF and storage medium is proposed by [36]. A conventional Rankine cycle is thermally driven by this solar energy system. The steam turbine's output flow, after being partially expanded, acts as the primary flow of a steam ejector. The discharge mixed flow is the heat source of the ORC unit. After heating the ORC system, this stream is split into two flows. One of them completes the Rankine cycle and the second flow is used for a preliminary preheating of the RO feedwater and subsequently for cooling production. The cooling of the ORC is also carried out with the feedwater of the desalination unit to obtain additional heating. Therefore, in this proposal, the ORC is not directly heated by the solar thermal plant.

2.1.2. Low-Temperature Solar Systems

The other option commonly addressed in recent studies is the combination of solar ponds (SPs) and a low-temperature ORC unit (see Figure 3) to power a RO desalination

system. The concept is not new; two of such systems were implemented in the USA—Los Baños (California) and El Paso (Texas) [37]. A solar pond is integrated in the same device for both solar–thermal energy conversion and long-term heat storage. With adequate procedures of creation and maintenance, three zones with different salinities remain throughout the lifetime of the SP. Thanks to the solar heating, thermal energy reaches the lowest layer (lower convective zone), consisting of high salinity solution. On top, a layer with an appropriate salinity gradient is created, so-called the non-convective zone (NCZ). Due to the corresponding density profile, its salinity gradient avoids convection in order to maximize the thermal insulation of the LCZ. The upper layer (upper convective zone, UCZ) provides insulation from the atmospheric phenomena. As Figure 3 depicts, solar heat is extracted from the lower convective zone (LCZ) of the SP, whereas the heat rejected by the ORC is re-injected into the upper convective zone (UCZ).
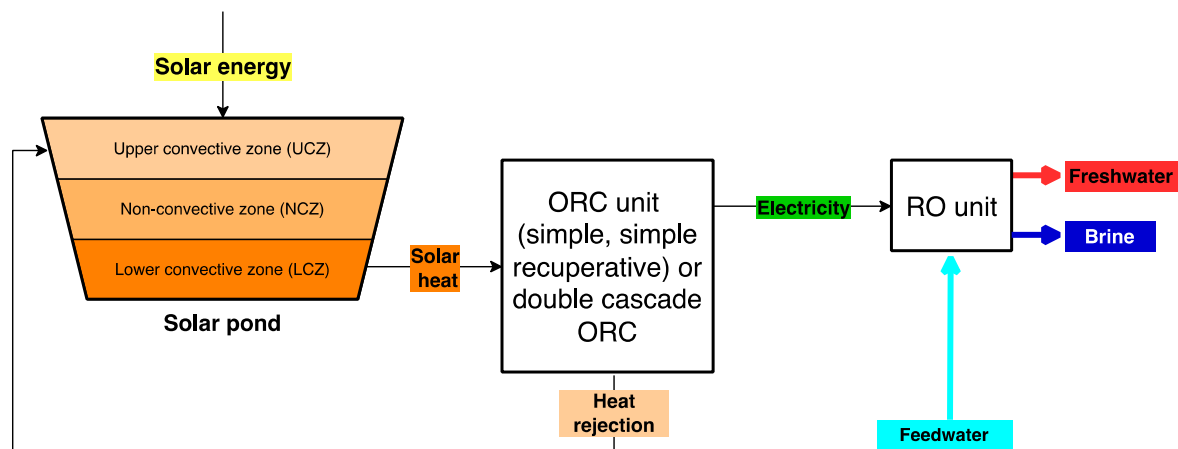

Figure 3. General scheme of solar-pond-driven RO desalination proposals.

The investigation of a solar RO desalination system using an SP that provides thermal energy to a recuperative ORC unit is presented by [38]. For this purpose, an HTF is used to extract energy from the lower convective zone. This HTF is circulated through the ORC evaporator. As for the desalination system, the feed water is first preheated in the ORC condenser and then circulated into the upper convective zone of the solar pond before entering the desalination unit. The brine stream from the RO unit is partially evaporated and a portion is subsequently injected into the lower convective zone in order to replenish salts losses due to their diffusion to the upper layers. The seawater RO unit is electrically driven by the ORC.

A RO desalination system based on a solar ORC powered by an SP is also presented in [39]. This configuration is proposed together with the analogous system, in which the ORC is replaced by a Kalina cycle. In the solar ORC configuration, an extracted fluid stream forms the LCZ and is circulated to the ORC evaporator, which incorporates recuperation. Part of the electrical power produced is used in the desalination unit while the rest is injected into the grid. It the use of the heat from the ORC condenser is also contemplated for a thermoelectric generation (TEG) system. A flow extracted from the upper convective zone is used as a cold sink for the TEG and re-injected into the upper convective zone after being heated. Seven different working fluids are considered for the ORC, resulting in an overall system exergy efficiency of up to 46.4% when using R227ea.

The double cascade concept is considered in the three designs investigated by [40], one of them without ORC, where an SP acts as the heat source of the topping cycle. The thermodynamic and thermoeconomic analysis of three configurations is performed. In two of them, a single ORC is thermally driven with energy extracted from the LCZ of the SP. The electricity output of this ORC is consumed by the RO unit. The heat rejection of the topping cycle is used as heat absorbed by the bottoming cycle, which, in one of the configurations,

is a Kalina cycle, and in the other, a simple ORC. In both cases, the cooling of the bottom cycle's condenser is carried out with water from the UCZ of the SP. A thermodynamic and thermoeconomic analysis is performed, assuming a SP surface area of 10,000 m^2, a temperature of 90 °C in the LCZ, and a RO unit conversion of 30% for seawater salinity of 42,485 g/kg.

2.2. Integration of Thermal Processes as Desalination Technology

When a thermal desalination process is considered to be integrated with a solar ORC system, recent proposals have mostly matched the layout shown in Figure 4. As can be seen, the integration implies the use of the heat rejected by the ORC to drive the thermal desalination process, which, in most of the proposals, involves a MED or MED-TVC unit. There are also some proposals with HDH or an MSF unit. Those desalination processes are described below.
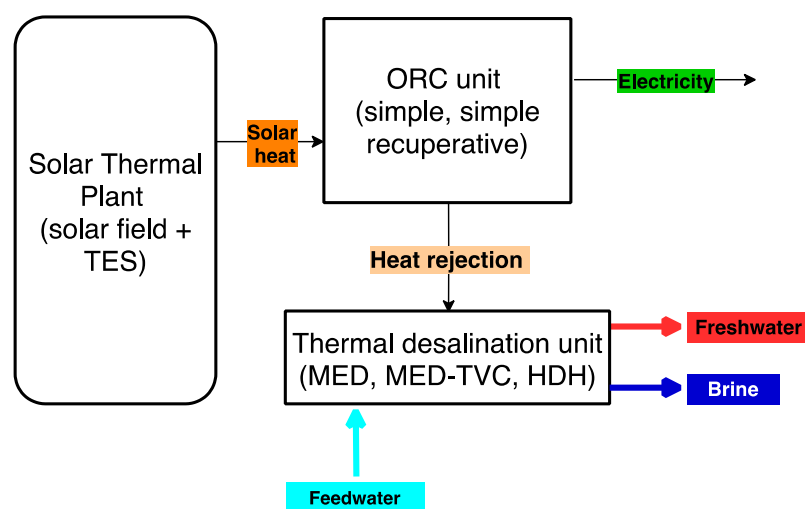

Figure 4. Integration of thermal desalination processes in solar-ORC-based poly-generation systems.

The industrial standard of the MED process comprises a MED unit coupled to a thermocompressor, as follows:

- MED unit. A set of several chambers (so-called effects) are kept under vacuum conditions with decreasing pressures, corresponding to the saturation pressure at decreasing temperatures from 50 to 67 °C, up to 45–35 °C. Normally there is a single heat exchanger consisting of a horizontal tube bundle and the evaporator. An external flow, providing the external heat source of the MED process, circulates within the evaporator tubes of the first effect. Seawater feed with slight preheating is sprayed on the surface of the tube bundle, thus resulting in a thin film that is partially evaporated. The remaining brine is discharged by the bottom of the effect, whereas the steam generated is sent to circulate inside the tubes of the evaporator of the next effect. The steam generated in the last effect is condensed in the end condenser. A seawater flow circulates through the end condenser; part of this flow (seawater cooling) is discharged back to the sea and the rest of the flow is the preheated seawater that enters all effects in parallel. Industrial plants normally have 8–12 effects in MED units and 4–8 effects in MED-TVC, although designs with 14 effects are feasible, with an average of around 2.5 °C of temperature gradient between adjacent effects. With 14 effects, the thermal energy consumption would be about 230 kJ/kg in a MED unit and 166 kJ/kg in MED-TVC.
- Termocompressor. A high-pressure steam flow (motive steam) is mixed with a low-pressure steam flow, thus resulting in a steam flow with intermediate pressure and temperature. This outlet steam flow drives the MED process: the low-pressure flow is the steam generated at the last effect or one of the last effects, whereas the motive

steam is generated by the available heat source. In conventional MED-TVC plants, the motive steam is a turbine extraction. Steam at about 140–225 °C is required in MED-TVC plants. Coupling the thermocompressor to the MED plant at the last effect makes the end condenser unneccesary. This results in avoiding the seawater cooling flow that requires significant electricity consumption, along with increased capital cost attributable to seawater intake infrastructure and pumps.

Moreover, MSF plants rely on steam generation due to the quick reduction of the pressure (flash) of the saline solution heated by an external heat source. An MSF plant consists of many flash chambers, the so-called stages, connected in series with a tube bundle (condenser) at the top. Steam generated in the process preheats the seawater feed as it circulates within the condenser tubes. After being preheated, seawater enters an external heat exchanger (brine heater) driven by the external heat source. Industrial plants include brine recycling since only a small portion of steam is generated. Then, brine, instead of seawater, suffers successive flash processes within the flash chambers, coupled in series. Condensers of several stages at the tail are cooled by an external seawater cooling flow. MSF plants exhibit very high auxiliary energy consumption, attributable to the cooling flow, the vacuum system, and the large flow of brine circulating through the flash stages.

Finally, the HDH process is based on increasing the relative humidity of the air by means of spraying water within an air flow at the humidifier. At least one of those flows, water and/or air, should be previously heated by an external heat source. Finally, at the dehumidifier, part of the steam within the hot moist air is condensed on the outer surface of colling tubes, thanks to the circulation of a cooling flow. Water and air circuits can be either open or closed. Moreover, their circulation can be forced or natural.

A solar poly-generation scheme is presented in [41]. The ORC unit with o-Xylene as the working fluid is powered by a solar thermal plant with PTCs (Sky Trough model) and a sensible TES. In both systems, Therminol VP-1 is used as the thermal fluid. The heat rejected by the ORC drives the MED unit and a single-effect absorption refrigeration system. The system is studied from energetic and exergetic points of view.

The use of a recuperative ORC unit driven by a solar thermal plant with PTC and TES, both with thermal oil as the thermal fluid, is proposed by [42], among other options. This configuration is compared with the analogous system comprised of a conventional Rankine cycle and molten salts as HTF and storage medium. In both cases, a MED plant is considered.

A system based on a solar thermal plant with PTCs and TES with thermal oil as the HTF and storage medium to drive an ORC unit is analyzed in [43,44]. N-octane is the working fluid. The electricity produced by the ORC is consumed in an electrolyzer for hydrogen production. The heat rejected by the ORC is used in an HDH desalination unit and also to preheat the desalinated water output, which will be consumed by the electrolyzer.

A solar poly-generation system to meet the cooling and water demands of a greenhouse is studied in [45]. The solar thermal plant with PTCs and TES provides thermal energy to an ORC unit and an absorption cooling system. Part of the electricity produced by the ORC—with toluene as the working fluid—is used in an electrolyzer, while the heat rejected is used to drive an MSF plant. The desalinated water is then used both in the electrolyzer and as a supply for the greenhouse. The oxygen and hydrogen produced are stored to produce backup thermal energy during periods of no solar radiation using a hydro-oxy combustor.

A solar poly-generation system based on an ORC unit integrating a steam ejector placed at the turbine's outlet is analyzed in [46]. The discharge mixed flow of the ejector is condensed with seawater, while the secondary flow of the ejector is previously used for cooling production. A MED plant fed with the vapor from an extraction at the ORC turbine is proposed as the desalination unit. Seawater is considered as the heat transfer fluid in the solar thermal plant.

In addition to the above, there are other recent proposals in the literature that do not match the scheme of Figure 4 but incorporate ORC units to supply the energy demanded

by a thermal desalination process. Examples of this are the proposals where the waste heat recovered from the exhaust gas of a gas turbine is used to supply heat to the ORC [47,48].

A compressed air energy storage (CAES) system to consume electricity during the off-peak hours of electrical demand is proposed by [47]. An intercooled two-stage compression process is considered, and aftercooling prior to storage also takes place. The heat recovered in both processes is used in the production of domestic hot water. During peak demand hours, the stored compressed air is used to produce electricity by means of a gas turbine. Prior to its combustion chamber, the air is preheated in a solar dish system. The exhaust gases from the turbine are used to supply the heat demanded by the simple cycle ORC unit, with toluene as the working fluid. The condenser of this unit is cooled with a MED plant. A 10 m diameter solar dish and a 6-effect MED plant with a top brine temperature of 70 °C and a feed of 40,000 ppm are analyzed. The results indicate an ORC output of 17.4 kW and 2.5 m^3/day of freshwater production with an overall exergy efficiency of 41.7%. As a storage system, the calculated configuration has a round trip efficiency of 65.2%. Two multi-objective optimizations with evolutionary algorithms are also performed by [47], resulting in optimal exergy efficiencies of around 51%.

A poly-generation system composed of a solar/fossil hybrid recuperative gas turbine cycle with an intercooled two-stage compression system is proposed in [48]. The air coming from the recuperator is solar-heated before entering the combustion chamber. The exhaust gases from the gas turbine are used to drive the ORC unit. Moreover, there is an absorption refrigeration system and a desalination unit, which consists of a single-stage flash process. The seawater feed is preheated in the ORC condenser and then within the condenser of the desalination unit. After being preheated, the seawater flow is separated into two streams. One of them is directly sent to the condenser of the refrigeration system. The second acts as the cooling flow of the two-stage compression before entering the refrigeration system, passing through the generator. The latter finally enters the desalination unit as feed water. At the outlet of the flash unit, the brine is air-cooled for low-grade heat production. For the thermodynamic analysis, concentrating solar collectors are considered, while R134a is the working fluid in the simple ORC. The proposed multi-generation configuration has an exergy efficiency of 27%. This configuration is compared with another in which the solar hybrid gas cycle configuration is maintained but the ORC, cooling, and desalination systems are replaced by a Kalina cycle.

2.3. Proposals with Integration of Hybrid RO/Thermal Desalination

Recent hybrid desalination configurations with a solar-driven ORC unit can also be found in specific literature.

A solar–wind hybrid system, in which a simple solar ORC operated with toluene is connected to a solar parabolic trough field without TES, is presented in [49]. In addition to the ORC, electricity production from a wind turbine is also considered. The total electricity output drives a seawater RO desalination plant and the surplus is sold to the grid. The rejected heat of the ORC is also used in a MED-TVC plant.

Jaubert et al. [50] present the analysis of three RO-MED hybrid solar desalination systems powered by a PTC field without TES. Therminol VP-1 is selected as the heat transfer fluid. Part of the RO brine flow is used in the MED plant. As for the ORC, two possible working fluids are considered in this work. On one hand, there is isopentane, a fluid usually considered in ORC studies, and on the other hand, ethyl butyrate, which represents a case not studied so far and, according to the authors, shows promising results. In the three proposed configurations, the heat rejected by the ORC preheats the feed water of the reverse osmosis unit and the brine flow of the reverse osmosis unit before it enters the MED plant. As for the ORC architectures, the simple cycle, simple regenerative and simple regenerative, and solar reheating of the vapor are considered.

3. Solar sCO$_2$ Power Cycle and Desalination

Xia et al. [51] propose a solar-powered transcritical CO$_2$ Rankine cycle for RO desalination based on the recovery of the cryogenic energy of liquefied natural gas (LNG). The use of the LNG as the cold sink ($-161\,^\circ$C) allows the condensation of the CO$_2$. The solar thermal system is composed of a compound parabolic concentrator (CPC) solar field and a thermal energy storage system with thermal oil as an HTF and storage medium. Regarding the power cycle, seawater is considered the hot fluid in the preheater of the Rankine cycle. A sensitivity analysis was performed in [51] to investigate the effect of several parameters on the daily values of exergy efficiency and net mechanical work and freshwater outputs. Afterwards, the multi-objective optimization of the system by means of a genetic algorithm was also performed. The optimized system, with a total aperture area of CPC collectors of 235 m^2 and a seawater RO unit with a feedwater salinity of 45 kg/m^3, exhibited a daily exergy efficiency of 4.90% and a freshwater output of 2537 m^3.

Additionally, the next table (Table 1) summarizes recent proposals of desalination systems integrated into power cycles operated with CO$_2$, most of them dealing with Brayton cycles operated with supercritical CO$_2$ (sCO$_2$), as reported below. The top temperatures needed by sCO$_2$ to achieve high energy efficiency require point-focusing solar concentration along with two-axis sun tracking. At the industrial scale, a heliostat solar field focuses solar irradiance on the solar receiver placed on top of a tower. Either the storage medium or the working fluid would be heated as it circulates through the solar receiver. Plants with this technology are called solar tower power plants or central receiver solar plants, regardless of the power cycle implemented. Conventional concentrated solar power (CSP) plants are based on either, solar tower technology, or a Rankine cycle with water driven by a PTC solar field. Recent CSP plants have normally used sensible TES, consisting of two tanks of molten salts.

Table 1. Recent solar CO$_2$-based power-cycle-driven desalination proposals.

Reference	Solar Technology	Thermal Energy Storage	Supercritical CO$_2$ Power Cycle	Desalination Technology
[51]	CPC	Sensible—Thermal oil	Simple	SWRO
[52]	Solar tower	Sensible—Two tanks molten salt	Recuperated	MED-TVC
[53]	Solar tower	Sensible—Two tanks molten salt	Recompression	MED-TVC
[34]	Solar tower	Sensible—Two tanks molten salt	Recompression	MED
[54]	Solar tower	Sensible—Two tanks molten salt	Recompression	MED
[55–57]	Solar tower	Sensible—Two tanks molten salt	Recuperated+ Recompression	MED

Kouta et al. [52,53] studies the integration of solar tower (or central receiver) technology with supercritical CO$_2$ and MED-TVC desalination, with a top temperature of around 460 $^\circ$C. Two different configurations—recompression and recuperated—of the power cycle are considered, and a two-tank molten salt TES system is also included. In both cases, the MED-TVC plant is powered by the hot storage tank instead of the heat rejected by the sCO$_2$ power cycle. Therefore, the hot storage tank drives both the power cycle and the generation of the motive steam of the thermocompressor of the MED-TVC plant. This layout corresponds to a desalination system directly driven by solar energy. All the subsystems are modeled for thermodynamic performance, which is carried out for six different cities in Saudi Arabia.

Yuan et al. [34] also present a configuration based on a central tower system with storage by means of two molten salt tanks. The heat rejected in the cooler of a CO$_2$ Brayton cycle with recompression and regeneration is used to produce steam for the MED plant, with a top brine temperature of 70 $^\circ$C. Optimization of the configuration yields a solar

power cycle efficiency of 24% and the coupling of the same with a 5-effect MED plant with a capacity of 459 m^3/d.

Omar et al. [54] presented an interesting analysis of the CSP plant with the sCO$_2$–MED combination. The origin of their approach is the inability to use more than 25% of the total waste heat rejected by the cycle with the MED plant in previously proposed designs. To overcome this value, the use of a cascade design of MED plants was proposed for the first time. A cost–benefit analysis was also carried out regarding the location of the CSP-MED system, given the reduction in the solar resource available when moving the plant closer to the coastline. In the proposed configuration, part of the heat rejected by the sCO$_2$ recompression cycle is utilized by a cascade of MED plants. The result of the analysis concludes that with a 4 MED plant cascade, it is possible to recover up to 57% of the total waste heat of the cycle, whereas the levelized cost of water is minimized with a cascade of 3 MED plants. Another interesting conclusion is that the influence of the power cycle on the payback period is considerably higher than that of the desalination system.

Finally, Sharan et al. [55] carried out a design parameter selection of a MED system to be coupled to a sCO$_2$ cycle with recuperation and recompression, considering 600 °C as the maximum temperature. Moreover, in [56], the authors proposed an innovative MED configuration to better exploit the waste heat resource. The analysis of the full solar system in different plant locations is reported in [57], considering a turbine inlet temperature of 554 °C, which is suitable for the selected energy storage medium. It is worth noting that the author considered phase change materials to partially store the heat rejected by the power cycle in order to maximize the operating hours of the desalination unit with minimum investment cost.

4. Assessment of Innovative Configuration of CSP + D Plants

The assessment of main issues to draw conclusions concerning design recommendations of CSP + desalination (CSP + D) plants are summarized below:

1. There is an important number of proposals of solar ORC systems in which desalinated water is produced by means of a thermal process that receives the heat discharged by the cycle. The most common technology is MED, although it is also possible to find some designs with HDH. First, auxiliary consumption of thermal desalination processes should be taken into account in comparison to that of RO desalination, as Section 4.1 describes. Second, the coupling of thermal desalination to an ORC requires an increase in condensing temperature. This results in the lower energy efficiency of the ORC in thermal desalination applications, which should be compared to ORC/RO desalination (see Section 4.2).

2. Concerning solar ORC-RO technology with a solar thermal system in the medium-temperature range, most designs focus on PTCs and thermal storage in addition to the use of the heat rejected by the cycle for other processes, mainly cooling by single-effect absorption. The use of this heat for the preheating of the RO feed water is also considered. The assessment of poly- or multi-generation schemes in solar ORC, including cooling applications, requires further analysis focused on the effect of condensing temperature of the power cycle, presented in Section 4.2. Moreover, the proposed seawater preheating should be assessed case by case, having regard to regulations of product quality since a temperature increase makes the compliance of boron content difficult. Further treatment of product water could be required, thus increasing capital and operation expenses. Therefore, no general conclusion can be pointed out in this regard.

3. When low-temperature ORC is considered to drive the RO, the most common option is a solar pond being used as a solar thermal collector and storage system. In this case, heat is supplied to the ORC from the lower convective zone of the SP and the upper convective zone is the cold sink. The combined system SP/ORC/RO exhibits the highest solar energy consumption in comparison to any other solar desalination technology [7]. However, this option is inexpensive due to three main reasons: the

RO desalination system can operate 24 h/day most of the year, no additional energy storage is required, and the low cost of the SP technology.

4.　In relation to the coupling of desalination processes with solar sCO_2 cycles, it has been noted that there are few design proposals to date. Most of them correspond to the use of the heat rejected by the cycle to drive MED plants. As a common feature in all of them, not all the waste heat of the cycle contributes to the desalination process. The coupling of thermal desalination and solar power cycles based on sCO_2 has a lower effect on the cycle efficiency than that of solar ORCs. Innovative configurations of MED plants, such as those proposed by Omar et al. [54] and Sharan et al. [56], have significant market prospects as cost-effective solutions. However, Sharan et al. [56] reported on maximum freshwater production of about 2500 m^3/d in a solar sCO_2 plant of 115 MW of net power output. This means a ratio of desalination production to power output of 21.7 m^3/d/MW, so higher water demands should be provided by RO desalination.

4.1. Auxiliary Energy Consumption in Thermal Desalination

The energy balance over a thermal desalination process as a whole allows the calculation of the seawater cooling required in addition to the feed flow. Figure 5 depicts the ratio of mass flow rates of cooling to product as a function of the specific thermal energy consumption (STEC) of the distillation process, corresponding to four different temperature increases, ranging from 5 to 20 °C. The selection of this parameter depends on local regulations regarding the maximum temperature increase of flows discharged back to the sea. An ambient temperature of 20 °C and seawater salinity of 0.035 kg of salts per kg of seawater are considered. The STEC of industrial MED plants normally ranges from 230 to 330 kJ/kg, considering a well-known dependence on the number of effects. However, MED units studied in the literature of ORC and sCO_2 mostly exhibit higher STEC, up to 575 kJ/kg or even more. Moreover, HDH processes consume between 575 and 2300 kJ/kg of STEC, whereas the STEC of a single flash chamber corresponds to around 2300 kJ/kg. According to Figure 5, design proposals should take into account extra costs attributable to cooling flow, namely, capital expenses of seawater intake and pumping systems, along with pumping electricity consumption.
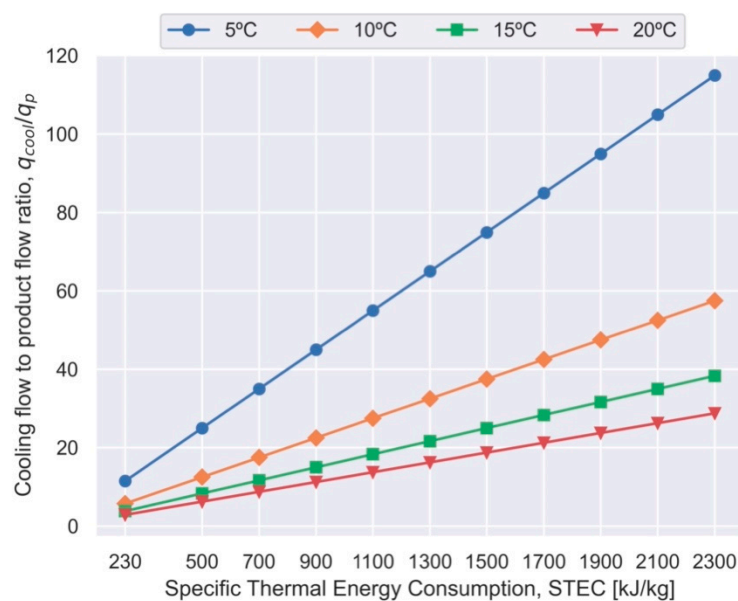

Figure 5. Ratio of cooling flow (q_{cool}) to product flow (q_p) versus the specific thermal energy consumption (STEC) of a thermal desalination plant, considering a temperature increase of the colling flow from 5 to 20 °C.

4.2. Effect of Condensing Temperature in Medium-Temperature ORCs

This section presents a comparative analysis of medium-temperature solar desalination system configurations with ORCs, in which the heat rejected by the cycle is used in a thermal desalination process or absorption cooling. In this way, it is possible to evaluate the effect of increasing the condensing temperature of the ORC on the cycle itself and also on the solar field and thermal storage. This analysis is not usually found in the specific literature where such variants are proposed.

The basic layout considered for a CSP − ORC plant with thermal storage is shown in Figure 6. The solar field could be composed of PTCs or linear fresnel reflectors (LFRs), and the TES can consist of a direct two-tank system or a single thermocline tank, either with liquid or solid filler (packed-bed system). A thermal oil is used as the HTF. This type of plant has been evaluated by several authors [58–62].
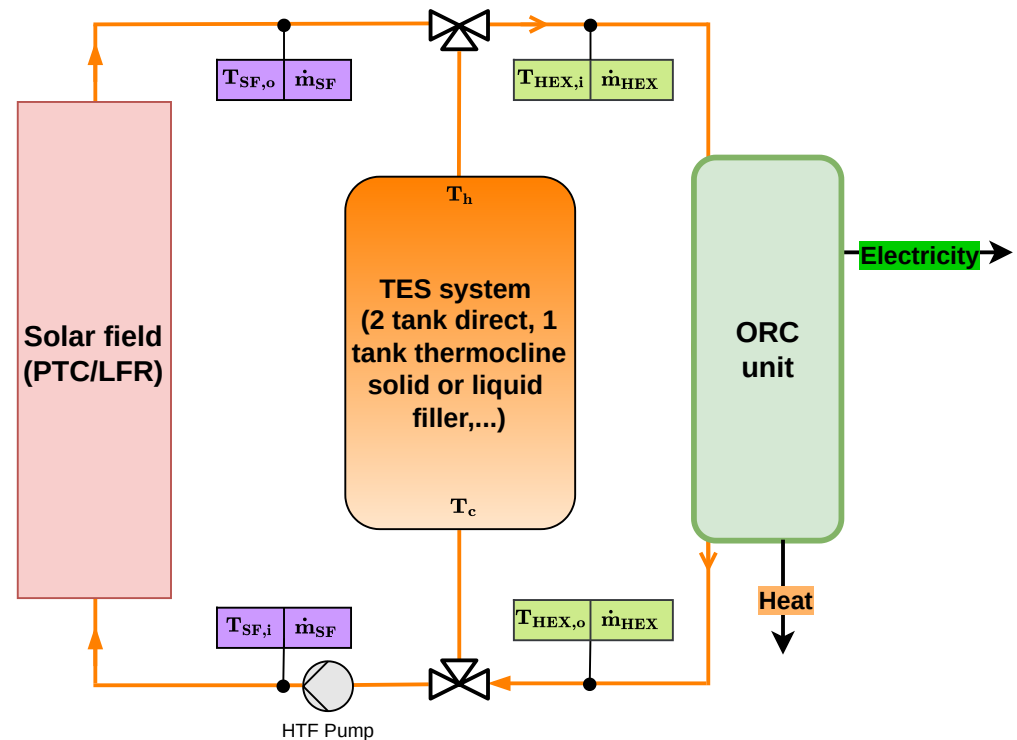

Figure 6. Reference plant configuration (CSP-ORC).

Table 2 shows the input parameters that determine the performance of the ORC and the final thermal oil loop temperature. With the chosen ORC's working fluid (MDM) and the parameters set, performance values of commercial ORC units operating with thermal oil at 300 °C as the thermal source are close to reproducing it, both in the power-only (about 25%) and CHP (about 18–19%) modes [63]. For the simplicity of the analysis, the thermal losses between the solar field's outlet and the solar heat exchangers' inlet are considered negligible, such that $T_{SF,i} = T_c = T_{HEX,o}$ and $T_{SF,o} = T_h = T_{HEX,i}$.

As shown in Figure 7, increasing the condensing temperature of the ORC to allow the use of the rejected heat implies a significant reduction in its thermal efficiency or, equivalently, an increase in the available heat per unit of net power output. An increase in the final cooling temperature of the thermal oil ($T_{HEX,o}$) is also observed, which does not favor the sizing of the TES or the performance of the solar field.

To estimate the effect on storage sizing, two options commonly discussed in the literature are considered [58,60,62]: direct storage with the HTF itself, e.g., using a two-tank

system, and single tank thermocline storage with solid filler. The basic sizing in both cases can be calculated using the following expression [58]:

$$V_{TES} = \frac{E_{TES}}{(1 - \epsilon) \times \rho_s \times c_s \times (T_h - T_c) + \epsilon \times \rho_l \times \Delta h_l} \tag{1}$$

where E_{TES} is the nominal energy capacity of the storage, and ϵ is the void fraction (liquid volume to total volume ratio). The properties of liquid density (ρ_l) and enthalpy (Δh_l) were determined using the CoolProp library [64,65], taking the density at the average temperature $(T_h + T_c)/2$. As for the void fraction, its value has been estimated in the order of those used by [59,62,66,67]. Density (ρ_s) and heat capacity (c_s) values for the solid filler have also been chosen according to [66].

Table 2. Information used to compute the ORC's performance, HTF-ORC heat exchange processes, and basic sizing of the TES.

| ORC	
Working fluid	MDM (octamethyltrisiloxane)
Recuperator effectiveness	0.7
Evaporation temperature, T_{evap}	270 °C
Feed pump's isentropic efficiency, η_P	0.75
Turbine's isentropic efficiency, η_t	0.85
Secondary HTF loop	
Heat Transfer Fluid	Therminol VP-1
Temperature at solar heat exchangers inlet, $T_{HEX,i}$	300 °C
Temperature difference at solar heat exchangers inlet	15 °C
Pinch point	10 °C
Thermal energy storage (TES)	
Liquid storage medium	Therminol VP-1
Heat capacity of solid storage medium, c_s	850 J/(kg × K)
Density of solid storage medium, ρ_s	2600 kg/m^3
Void fraction	0.30
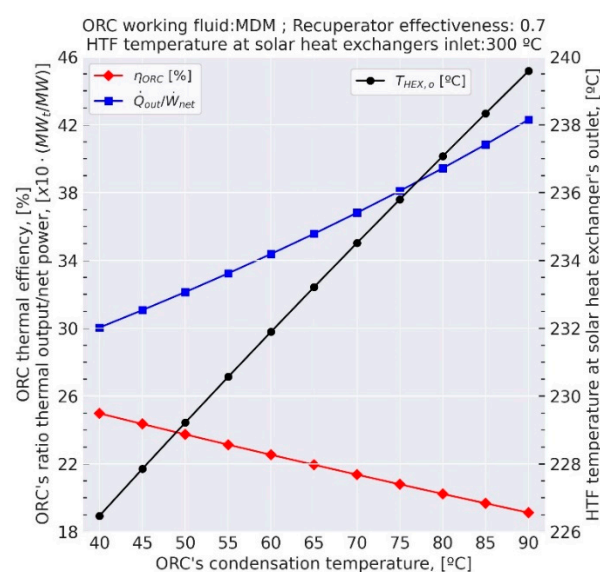
Figure 7. Effect of the ORC's condensation temperature on thermal efficiency, heat output to net power output ratio, and HTF's temperature at the solar heat exchangers' outlet.

Figure 8 shows the effect of the ORC's condensation temperature (T_{cond}) on the required volume of storage medium per unit of stored energy. As expected, increasing T_{cond} implies a larger required storage volume since the hot–cold temperature difference to which the storage medium is subjected is reduced. Because the CSP − ORC plant produces electricity to be used in the production of freshwater or cooling, the required volume of storage medium per unit of equivalent electrical energy stored is also depicted in Figure 8. With this parameter, the change of the ORC's performance is reflected over the storage volume.
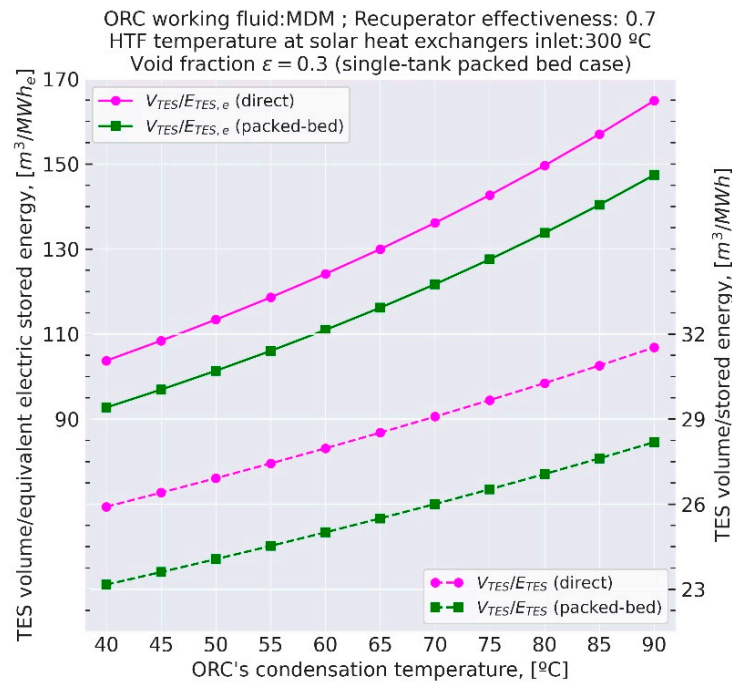

Figure 8. Storage medium volume per unit of stored energy as a function of the ORC's condensing temperature.

The performance of the solar field (SF) at the design conditions is estimated with a model widely used in the literature [58,60,62,68]. The efficiency of the solar field—thermal energy output to incident solar power ratio—is computed as the difference between the optical efficiency ($\eta_{0,SF}$) and thermal losses terms:

$$\eta_{SF} = \left(\frac{\dot{Q}_{SF,out}}{G_{b,N} \cdot A_{SF}} \right) = \eta_{0,SF} - \left(\frac{\dot{Q}_{SF,losses}}{G_{b,N} \cdot A_{SF}} \right) \tag{2}$$

where A_{SF} is the total area of the solar field.

For the comparison presented in this section, it is assumed that a solar field is composed of PTCs. In that case, the optical efficiency is computed by taking into account the shadow (η_{shadow}) and end losses ($\eta_{endloss}$), the cleanliness of the solar collectors (F_e), the availability of the solar field (av_{SF}), and the influence of the incidence angle (θ) on its peak optical performance ($\eta_{opt,0}$) via the incidence angle modifier (K):

$$\eta_{0,SF} = \eta_{opt,0} \cdot K \cdot F_e \cdot \eta_{shadow} \cdot \eta_{endloss} \cdot av_{SF} \tag{3}$$

On the other hand, thermal losses are modeled as:

$$\dot{Q}_{SF,losses} = \left[a_1 \cdot (\overline{T}_{SF} - T_{amb}) + a_2 \cdot (\overline{T}_{SF} - T_{amb})^2 \right] \cdot A_{SF} \tag{4}$$

where $\overline{T}_{SF}$ is the average inlet/outlet heating temperature of the HTF, and a_1 and a_2 are the heat losses coefficients. Values of these coefficients are derived from the information available at [69]. Parameters selected for the evaluation of the solar field performance at design conditions are given in Table 3. Two extreme values are considered for the a_1 coefficient to quantify the influence of the ORC's condensation temperature in scenarios of different solar-to-thermal energy conversion efficiency values. The two resulting curves are depicted in Figure 9.

Table 3. Location and design conditions for the efficiency computation of the PTC solar field.

| Location	Fuerteventura (Canary Islands, Spain)
Latitude, longitude	28.317–14.071°
Design conditions	
Ambient temperature, T_{amb}	23 °C
Direct normal irradiance, $G_{b,N}$	850 W/m^2
Peak optical performance, $\eta_{opt,0}$	075
Cleanliness index, F_e	0.97
Availability, av_{SF}	0.95
Design point	Solar noon, 21 June
Orientation	North-South (East-West tracking)
Incidence angle, θ	4.87°
Optical efficiency, $\eta_{0,SF}$	0.67
Heat losses coefficient, a_1 (low–high value)	0.02–0.4 W/m^2 × K
Temperature dependence of the heat loss coefficient, a_2	0.001 W/m^2 × K^2
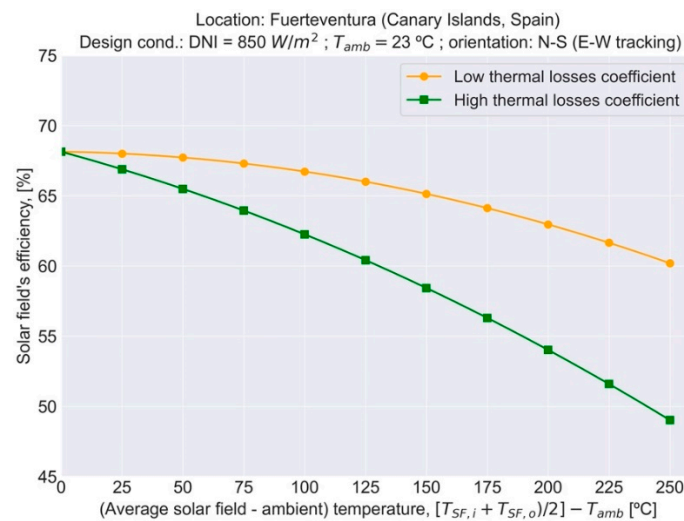
Figure 9. Solar field's efficiency according to the parameters fixed in Table 3.

Figure 10 shows the CSP − ORC + (MED + RO) configuration for which a condensation temperature of 70 °C is studied. To assess only the desalination application, the remaining net power output ($\dot{W}_{net}$) not consumed as auxiliary by the MED plant (Specific Electricity Consumption, (SEC_{MED}) is dedicated to an RO unit (SEC_{RO}). Under these assumptions, the volumetric flow rate of freshwater ($\dot{V}_p$) is computed with the following expressions:

$$\dot{V}_{p,MED} = \dot{Q}_{in} \cdot \frac{(1 - \eta_{ORC})}{STEC_{MED}} \tag{5}$$

$$\dot{V}_{p,RO} = \frac{\dot{W}_{net}}{SEC_{RO}} - \dot{V}_{p,MED} \cdot \left(\frac{SEC_{MED}}{SEC_{RO}} \right) \tag{6}$$

This configuration is compared with the one shown on the left side, for which a condensing temperature of 40 °C is assumed and whose net power produced is fully consumed by an RO unit. In this case, $\dot{V}_{p,RO}$ can also be computed with the expressions above, making $\dot{V}_{p,MED} = 0$. Table 4 shows the numerical results of the comparison, assuming the same total desalination capacity in both cases.
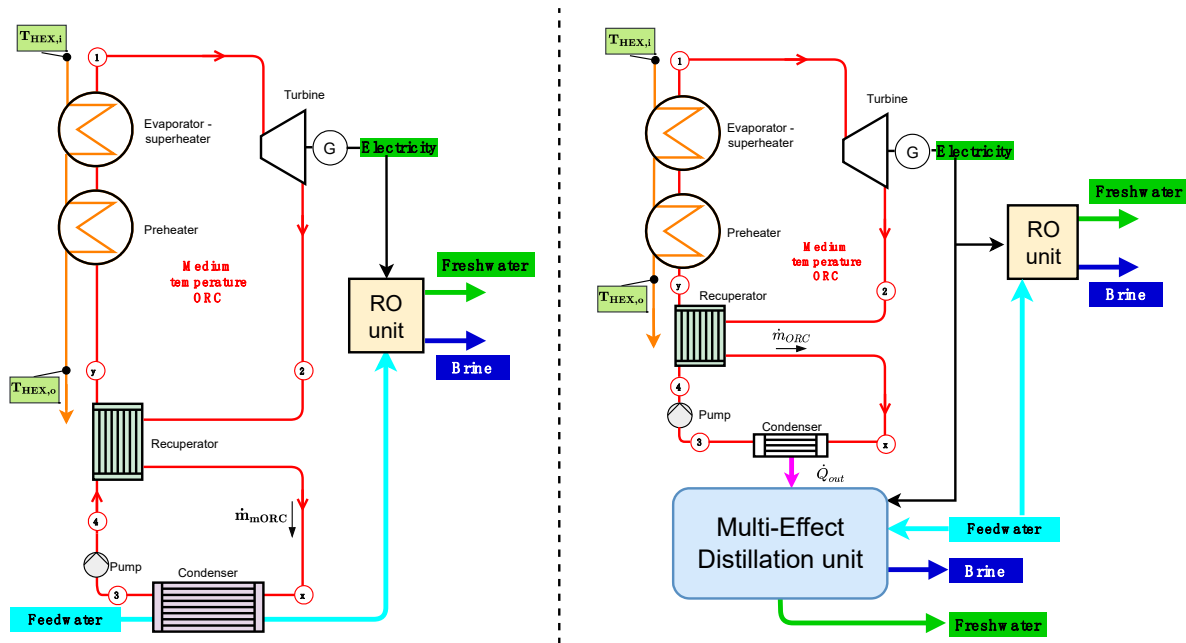

Figure 10. Configurations considered to be compared: CSP − ORC + RO (**left**) and CSP − ORC + (RO + MED) (**right**).

Table 4. Comparison of the CSP − ORC configuration for desalination (same desalination capacity). SEC_{RO} = 3 kWh/m^3; SEC_{MED} = 2 kWh/m^3; PR = 10. Direct TES with thermal oil Therminol VP-1.

	CSP − ORC + RO		CSP − ORC + (MED + RO)	
ORC's condensation temperature, T_{cond}	40 °C		70 °C	
ORC's evaporation temperature, T_{evap}	270 °C		270 °C	
ORC's thermal efficiency, η_{ORC} [%]	24.98		21.37	
HTF's outlet temperature, $T_{HEX,o}$	226.5		234.5	
Average solar field temperature [°C]	263		267	
Solar field's efficiency, η_{SF} (low a_1/high a_1)	0.608	0.501	0.606	0.500
Storage medium volume/stored energy [m^3/MWh]	25.9		29.1	
Storage medium volume/equivalent electric stored energy [m^3/MWh$_e$]	103.7		136.1	
ORC thermal input/total desalination capacity [kW/(1000 m^3/day)]	500		554	
Net ORC power output/total desalination capacity [kW/(1000 m^3/day)]	125		118	
Solar field's area (SM = 1)/total desalination capacity [m^2/(1000 m^3/day)] (low a_1/high a_1)	968	1175	1075	1303
Storage medium volume (1 h)/total desalination capacity [m^3/(1000 m^3/day)]	13.0		16.1	

As can be seen, increasing the condensing temperature to 70 °C to include the MED unit requires an ORC unit with less net power due to the utilization of the heat rejected by the cycle for freshwater production output (118 kW instead of 125 kW per 1000 m^3/day of capacity, 6% less). However, the negative effect of the above is clearly reflected in the solar field area and storage volume requirements. In the first case, 11% more area would be required for solar multiple (SM) = 1 due to the higher thermal energy input of the ORC unit, while in the second case, the increase would be 24%.

The configurations to be compared when the heat rejected by the cycle is consumed in the generator of an absorption cooling system are shown in Figure 11. To make the comparison consistent, a mechanical vapor compression (VC) refrigeration system is analyzed when the condenser's heat is not used for this purpose. For the CSP − ORC + (RO + ARS) configuration, the auxiliary electrical consumption of the absorption refrigeration unit is considered negligible, in which case, both the cooling capacity ($\dot{Q}_{c,AR}$) and the desalinated water flow rate ($\dot{V}_{p,RO}$) are easily computed as:

$$\dot{Q}_{c,AR} = COP_{AR} \cdot \dot{Q}_{in} \cdot (1 - \eta_{ORC}) \tag{7}$$

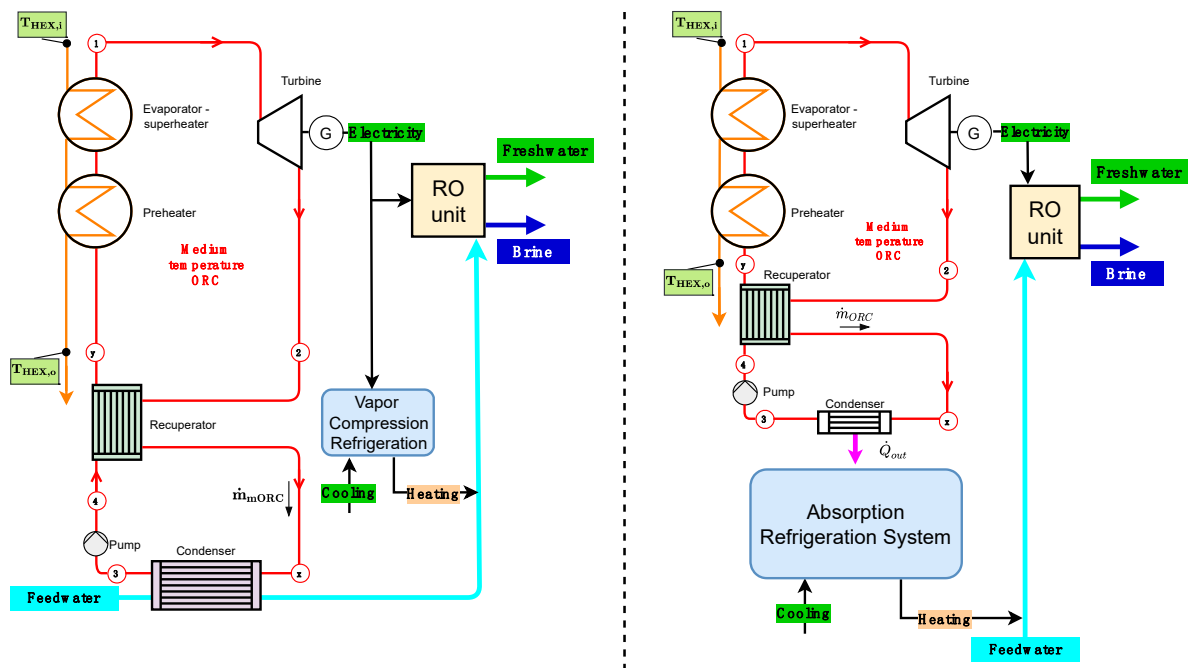$$\dot{V}_{p,RO} = \dot{Q}_{in} \cdot \frac{\eta_{ORC}}{SEC_{RO}} \tag{8}$$

Figure 11. Configurations considered to be compared: CSP − ORC + (RO + VC) (**left**) and CSP − ORC + (RO + ARS) (**right**).

For the CSP − ORC + (RO + VC) configuration, the $\dot{V}_{p,RO}$ can be obtained from:

$$\dot{V}_{p,RO} = \frac{1}{SEC_{RO}} \cdot \left[\eta_{ORC} \cdot \dot{Q}_{in} - \frac{\dot{Q}_{c,VC}}{COP_{VC}} \right] \tag{9}$$

where $\dot{Q}_{c,VC}$ is the cooling capacity of the vapor compression refrigeration system.

The numerical results of the comparison for the same cooling and desalination capacity are shown in Table 5, where a condensing temperature of 90 °C is assumed for the operation of the absorption refrigeration unit.

Table 5. Comparison of the CSP − ORC configuration for desalination and refrigeration (same desalination and cooling capacity). SEC_{RO} = 3 kWh/m³; direct TES with thermal oil Therminol VP-1.

	CSP − ORC + (RO + VC)		CSP − ORC + (RO + AR)	
ORC's condensation temperature, T_{cond}	40 °C		90 °C	
ORC's evaporation temperature, T_{evap}	270 °C		270 °C	
ORC's thermal efficiency, η_{ORC}	24.98%		19.12%	
HTF's outlet temperature, $T_{HEX,o}$	226.5 °C		239.6 °C	
COP	4		0.7	
Average solar field temperature [°C]	263		270	
Solar field's efficiency, η_{SF}	0.608	0.501	0.604	0.493
Solar field's area (SM = 1), A_{SF} [m²]	4553	5526	3440	4215
Storage medium volume/stored energy [m³/MWh]	25.9		31.5	
Storage medium volume/equivalent electric stored energy [m³/MWh$_e$]	103.7		164.9	
ORC thermal input/total desalination capacity [kW/(1000 m³/day)]	871		654	
Net ORC power output/total desalination capacity [kW/(1000 m³/day)]	218		125	
Solar field's area (SM = 1)/total desalination capacity [m²/(1000 m³/day)]	1685	2045	1273	1560
Storage medium volume (1 h)/total desalination capacity [m³/(1000 m³/day)]	22.6		20.6	

Unlike the use for MED desalination, the use of the condenser's heat for cooling combined with RO desalination has advantages over a configuration in which the cooling production is performed by a compression system to avoid increasing the condensation temperature of the cycle. Moreover, this situation is observed for a relatively high COP value of the compression chiller. Even in that case, the better performance of the ORC does not lead to a smaller size of the ORC unit, which finally implies a larger storage volume and a larger required solar field area.

5. Conclusions and Recommendations

The following trends have been detected after the update of the design proposals recently found in the specific literature on solar desalination systems based on ORCs. In the medium-temperature range, it is common to find proposals in which the heat rejected by the cycle is used, in general, to drive thermal desalination processes (mainly MED) or absorption cooling processes. In the low-temperature range, there are numerous proposals for the use of solar ponds as solar collection and energy storage systems. Regarding the coupling of desalination systems with solar supercritical CO_2 power cycles, the most common option is the use of the heat rejected by the cycle by means of MED units.

In addition, the critical analysis of the reviewed configurations leads to the following conclusions and design recommendations:

- In remote locations, solar desalination systems based on solar-pond-driven ORC/RO should be studied in comparison to solar PV/RO plants to supply only the freshwater demand.
- Concerning the selection of thermal desalination versus reverse osmosis, design proposals should consider the extra costs attributable to cooling flow, namely, capital expenses of seawater intake and pumping systems, along with pumping electricity consumption (see Figure 5).

- A comparative analysis of solar ORC/RO combined with cooling technologies has been performed. The use of the heat rejected by the cycle to drive an absorption refrigeration system is superior since results show that a bigger solar field and storage system would be needed to supply the same cooling capacity with a mechanical vapor compression refrigeration system (see Table 5).

- A comparative analysis has also been carried out to compare solar ORC/MED and solar ORC/RO desalination. Auxiliary electricity consumption of 0.75 kWh/m^3 is assumed in seawater RO desalination, attributable to the control system and feed pumping, whereas 2 kWh/m^3 has been considered in MED plants due to the additional requirements of a vacuum system and cooling flow pumping (see Figure 5). Results (see Table 4) show that thermal desalination is not recommended to exploit the heat rejection of the power cycle since the condensing temperature must be increased to couple the MED unit.

- On the contrary, heat rejection of sCO$_2$ cycles in CSP plants may be economically exploited by innovative MED desalination plants with the so-called cascade design depending on both local regulations of discharge temperature and the corresponding auxiliary pumping of cooling flow. Water production is limited to the waste heat available, so in the case of higher water demands, RO desalination is the only option recommended. Either seawater feed or concentrate flows of the RO plant can be used as the cooling flow of the power cycle, up to the maximum limit of temperature discharge.

Based on the results of the present literature update and assessment, research on the improvement of solar ORC configurations for poly-generation, with freshwater production through desalination, is considered a future work of interest, in addition to solar sCO$_2$ coupled to novel MED plants with enhanced energy efficiency.

Institutional Review Board Statement: Not applicable.

Informed Consent Statement: Not applicable.

Conflicts of Interest: The authors declare no conflict of interest. The funders had no role in the design of the study; in the collection, analyses, or interpretation of data; in the writing of the manuscript, or in the decision to publish the results.

References

1. International Energy Agency, IEA. Data and Statistics Page. Available online: https://www.iea.org/data-and-statistics/data-browser?country=WORLD&fuel=Energysupply&indicator=TESbySource (accessed on 31 October 2021).
2. The World Bank. DataBank. World Development Indicators. Available online: https://databank.worldbank.org/source/world-development-indicators (accessed on 31 October 2021).
3. Ihsanullah, I.; Atieh, M.A.; Sajid, M.; Nazal, M.K. Desalination and Environment: A Critical Analysis of Impacts, Mitigation Strategies, and Greener Desalination Technologies. *Sci. Total Environ.* **2021**, *780*, 146585. [CrossRef] [PubMed]
4. Lee, K.; Jepson, W. Environmental Impact of Desalination: A Systematic Review of Life Cycle Assessment. *Desalination* **2021**, *509*, 115066. [CrossRef]
5. Zapata-Sierra, A.; Cascajares, M.; Alcayde, A.; Manzano-Agugliaro, F. Worldwide Research Trends on Desalination. *Desalination* **2021**, *519*, 115305. [CrossRef]
6. Ghaffour, N.; Bundschuh, J.; Mahmoudi, H.; Goosen, M.F.A. Renewable Energy-Driven Desalination Technologies: A Comprehensive Review on Challenges and Potential Applications of Integrated Systems. *Desalination* **2015**, *356*, 94–114. [CrossRef]

7. Pouyfaucon, A.B.; García-Rodríguez, L. Solar Thermal-Powered Desalination: A Viable Solution for a Potential Market. *Desalination* **2018**, *435*, 60–69. [CrossRef]

8. Alnaimat, F.; Ziauddin, M.; Mathew, B. A review of recent advances in humidification and dehumidification desalination technologies using solar energy. *Desalination* **2021**, *499*, 114860. [CrossRef]

9. Alarcón-Padilla, D.C.; García-Rodríguez, L.; Blanco-Gálvez, J. Design recomendations for a multi-effect distillation plant connected to a double-effect absorption heat pump: A solar desalination case-study. *Desalination* **2010**, *262*, 11–14. [CrossRef]

10. Alarcón-Padilla, D.C.; García-Rodríguezz, L.; Blanco-Gálvez, J. Experimental assessment of connection of an absorption heat pump to a multi-effect distillation unit. *Desalination* **2010**, *250*, 500–505. [CrossRef]

11. Alarcón-Padilla, D.C.; Blanco-Gálvez, J.; García-Rodríguezz, L.; Gernjak, W.; Malato-Rodríguez, S. First experimental results of a new hybrid solar/gas multi-effect distillation system: The AQUASOL Project. *Desalination* **2008**, *220*, 619–625. [CrossRef]

12. Hassan, A.M. Fully Integrated NF-Thermal Seawater Desalination Process and Equipment Therefor. European Patent Application EP 1 614 660 A1, 9 July 2004.

13. Hassan, A.M. Fully Integrated NF-Thermal Seawater Desalination Process and Equipment. U.S. Patent US 20060157410, 20 July 2006.

14. Hassan, A.M. Process for Desalination of Saline Water, Especially Water, Having Increased Product Yield and Quality. U.S. Patent US 6508903, 21 January 2003.

15. Hassan, A.M.; Al-Sofi, M.A.K.; Al-Amoudi, A.S.; Jamaluddin, A.T.M.; Farooque, A.M.; Rowaili, A.; Dalvi, A.G.I.; Kither, N.M.; Mustafa, G.M.; Al-Tisan, I.A.R. A new approach to membrane and thermal seawater desalination processes using nanofiltration membranes (part 1). *Desalination* **1998**, *118*, 35–51. [CrossRef]

16. Wilf, M.; Awerbuch, L. *The Guidebook to Membrane Desalination Technology*; Balaban Desalination Publications: L'Aquila, Italy, 2007; ISBN 0-86689-065-3.

17. Palenzuela, P.; Zaragoza, G.; Alarcón-Padilla, D.C.; Guillén, E.; Ibarra, M.; Blanco, J. Assessment of different configurations for combined parabolic-trough (PT) solar power and desalination plants in arid regions. *Energy* **2011**, *36*, 4950–4958. [CrossRef]

18. Ortega-Delgado, B.; Palenzuela, P.; Alarcón-Padilla, D.C.; García-Rodríguez, L. Quasi-steady state simulations of thermal vapor compression multi-effect distillation plants coupled to parabolic trough solar thermal power plants. *Desalin. Water Treat.* **2016**, *57*, 23085–23096. [CrossRef]

19. Ortega-Delgado, B.; Palenzuela, P.; Alarcón-Padilla, D.-C. Parametric study of a multi-effect distillation plant with thermal vapor compression for its integration into a Rankine cycle power block. *Desalination* **2016**, *394*, 18–29. [CrossRef]

20. Hanafi, A.S.; Mostafa, G.M.; Waheed, A.W.; Fathy, A. I-D mathematical modeling and CFD investigation on supersonic steam ejector in MED-TVC. *Energy Procedia* **2015**, *75*, 3239–3252. [CrossRef]

21. Ameri, M.; Mohammadi, S.S.; Hosseini, M.; Seifi, M. Effect of design parameters on multi-effect desalinationsystem specifications. *Desalination* **2009**, *245*, 266–283. [CrossRef]

22. Mazini, M.T.; Yazdizadeh, A.; Ramezani, M.H. Dynamic modelling of multi-effect desalination with thermal vapour compressor plant. *Desalination* **2014**, *353*, 98–108. [CrossRef]

23. Kouhikamali, R.; Sanaei, M.; Mehdizadeh, M. Process investigation of different locations of thermo-compressor suction in MED–TVC plants. *Desalination* **2011**, *280*, 134–138. [CrossRef]

24. Esfahani, I.J.; Ataei, A.; Shetty, K.V.; Oh, T.; Park, J.H.; Yoo, C. Modeling and genetic algorithm-based multi-objective optimization of the MED-TVC desalination system. *Desalination* **2012**, *292*, 87–104. [CrossRef]

25. Temstet, C.; Canto, G.; Laborie, J.; Durante, A. A large high-performance MED plant in Sicily. *Desalination* **1996**, *105*, 109–114. [CrossRef]

26. Al-Mutaz, I.S.; Wazeer, I. Development of a steady-state mathematical model for MEE-TVC desalination plants. *Desalination* **2014**, *351*, 9–18. [CrossRef]

27. Fernández-Izquierdo, P.; García-Rodríguez, L.; Alarcón-Padilla, D.C.; Palenzuela, P.; Martín-Mateos, I. Experimental analysis of multi-effect distillation unit operated out of nominal conditions. *Desalination* **2012**, *284*, 233–237. [CrossRef]

28. Maurel, A. Dessalement et Energies Nouvelles. *Desalination* **1979**, *31*, 489–499. [CrossRef]

29. Libert, J.J.; Maurel, A. Desalination and Renewable Energies-a Few Recent Developments. *Desalination* **1981**, *39*, 363–372. [CrossRef]

30. Delgado-Torres, A.M.; García-Rodríguez, L.; Peñate, B.; de la Fuente, J.A.; Melián, G. Water Desalination by Solar-Powered RO Systems. In *Current Trends and Future Developments on (Bio-) Membranes: Renewable Energy Integrated with Membrane Operations*; Cassana, A., Figoli, A., Basile, A., Eds.; Elsevier: Amsterdam, The Netherlands, 2018; ISBN 978-0-12-813545-7. [CrossRef]

31. Ghermandi, A.; Messalem, R. Solar-Driven Desalination with Reverse Osmosis: The State of the Art. *Desalin. Water Treat.* **2009**, *7*, 285–296. [CrossRef]

32. Delgado-Torres, A.M.; García-Rodríguez, L. Design Recommendations for Solar Organic Rankine Cycle (ORC)-Powered Reverse Osmosis (RO) Desalination. *Renew. Sustain. Energy Rev.* **2012**, *16*, 44–53. [CrossRef]

33. Shalaby, S.M. Reverse Osmosis Desalination Powered by Photovoltaic and Solar Rankine Cycle Power Systems: A Review. *Renew. Sustain. Energy Rev.* **2017**, *73*, 789–797. [CrossRef]

34. Yuan, L.; Zhu, Q.; Zhang, T.; Duan, R.; Zhu, H. Performance evaluation of a co-production system of solar thermal power generation and seawater desalination. *Renew. Energy* **2021**, *169*, 1121–1133, Corrigendum in *Renew. Energy* **2021**, *172*, 632. [CrossRef]

35. El-Emam, R.S.; Dincer, I. Investigation and Assessment of a Novel Solar-Driven Integrated Energy System. *Energy Convers. Manag.* **2018**, *158*, 246–255. [CrossRef]
36. Tariq, S.; Safder, U.; Nguyen, H.T.; Ifaei, P.; Heo, S.K.; Yoo, C.K. A Novel Solar Assisted Multigeneration System Devoid of External Utilities for Drought Adaptation Considering Water-Exergy Nexus Analysis. *Appl. Therm. Eng.* **2021**, *198*, 117500. [CrossRef]
37. García-Rodríguez, L. Renewable energy applications in desalination: State of the art. *Sol. Energy* **2003**, *75*, 381–393. [CrossRef]
38. El Mansouri, A.; Hasnaoui, M.; Amahmid, A.; Hasnaoui, S. Feasibility Analysis of Reverse Osmosis Desalination Driven by a Solar Pond in Mediterranean and Semi-Arid Climates. *Energy Convers. Manag.* **2020**, *221*, 113190. [CrossRef]
39. Ghaebi, H.; Rostamzadeh, H. Performance Comparison of Two New Cogeneration Systems for Freshwater and Power Production Based on Organic Rankine and Kalina Cycles Driven by Salinity-Gradient Solar Pond. *Renew. Energy* **2020**, *156*, 748–767. [CrossRef]
40. Namin, A.S.; Rostamzadeh, H.; Nourani, P. Thermodynamic and Thermoeconomic Analysis of Three Cascade Power Plants Coupled with RO Desalination Unit, Driven by a Salinity-Gradient Solar Pond. *Therm. Sci. Eng. Prog.* **2020**, *18*, 100562. [CrossRef]
41. Kerme, E.D.; Orfi, J.; Fung, A.S.; Salilih, E.M.; Khan, S.U.D.; Alshehri, H.; Ali, E.; Alrasheed, M. Energetic and Exergetic Performance Analysis of a Solar Driven Power, Desalination and Cooling Poly-Generation System. *Energy* **2020**, *196*, 117150. [CrossRef]
42. Soliman, A.M.; Mabrouk, A.; Eldean, M.A.S.; Fath, H.E.S. Techno-Economic Analysis of the Impact of Working Fluids on the Concentrated Solar Power Combined with Multi-Effect Distillation (Csp-Med). *Desalin. Water Treat.* **2021**, *210*, 1–21. [CrossRef]
43. Delpisheh, M.; Haghghi, M.A.; Mehrpooya, M.; Chitsaz, A.; Athari, H. Design and Financial Parametric Assessment and Optimization of a Novel Solar-Driven Freshwater and Hydrogen Cogeneration System with Thermal Energy Storage. *Sustain. Energy Technol. Assess.* **2021**, *45*, 101096. [CrossRef]
44. Delpisheh, M.; Haghghi, M.A.; Athari, H.; Mehrpooya, M. Desalinated Water and Hydrogen Generation from Seawater via a Desalination Unit and a Low Temperature Electrolysis Using a Novel Solar-Based Setup. *Int. J. Hydrogen Energy* **2021**, *46*, 7211–7229. [CrossRef]
45. Mahmood, F.; Bicer, Y.; Al-Ansari, T. Design and Thermodynamic Assessment of a Solar Powered Energy–Food–Water Nexus Driven Multigeneration System. *Energy Rep.* **2021**, *7*, 3033–3049. [CrossRef]
46. Zhou, S.; Liu, X.; Feng, Y.; Bian, Y.; Shen, S. Parametric Study and Multi-Objective Optimization of a Combined Cooling, Desalination and Power System. *Desalin. Water Treat.* **2021**, *217*, 1–21. [CrossRef]
47. Javidmehr, M.; Joda, F.; Mohammadi, A. Thermodynamic and Economic Analyses and Optimization of a Multi-Generation System Composed by a Compressed Air Storage, Solar Dish Collector, Micro Gas Turbine, Organic Rankine Cycle, and Desalination System. *Energy Convers. Manag.* **2018**, *168*, 467–481. [CrossRef]
48. Hogerwaard, J.; Dincer, I.; Naterer, G.F. Solar Energy Based Integrated System for Power Generation, Refrigeration and Desalination. *Appl. Therm. Eng.* **2017**, *121*, 1059–1069. [CrossRef]
49. Makkeh, S.A.; Ahmadi, A.; Esmaeilion, F.; Ehyaei, M.A. Energy, Exergy and Exergoeconomic Optimization of a Cogeneration System Integrated with Parabolic Trough Collector-Wind Turbine with Desalination. *J. Clean. Prod.* **2020**, *273*, 123122. [CrossRef]
50. Jaubert, H.; Borel, P.; Guichardon, P.; Portha, J.F.; Jaubert, J.N.; Coniglio, L. Assessment of Organic Rankine Cycle Configurations for Solar Polygeneration Orientated to Electricity Production and Desalination. *Appl. Therm. Eng.* **2021**, *195*, 116983. [CrossRef]
51. Xia, G.; Sun, Q.; Cao, X.; Wang, J.; Yu, Y.; Wang, L. Thermodynamic Analysis and Optimization of a Solar-Powered Transcritical CO_2 (Carbon Dioxide) Power Cycle for Reverse Osmosis Desalination Based on the Recovery of Cryogenic Energy of LNG (Liquefied Natural Gas). *Energy* **2014**, *66*, 643–653. [CrossRef]
52. Kouta, A.; Al-Sulaiman, F.; Atif, M.; Marshad, S.B. Entropy, Exergy, and Cost Analyses of Solar Driven Cogeneration Systems Using Supercritical CO_2 Brayton Cycles and MEE-TVC Desalination System. *Energy Convers. Manag.* **2016**, *115*, 253–264. [CrossRef]
53. Kouta, A.; Al-Sulaiman, F.A.; Atif, M. Energy Analysis of a Solar Driven Cogeneration System Using Supercritical CO_2 Power Cycle and MEE-TVC Desalination System. *Energy* **2017**, *119*, 996–1009. [CrossRef]
54. Omar, A.; Saldivia, D.; Li, Q.; Barraza, R.; Taylor, R.A. Techno-Economic Optimization of Coupling a Cascaded MED System to a CSP-SCO$_2$ Power Plant. *Energy Convers. Manag.* **2021**, *247*, 114725. [CrossRef]
55. Sharan, P.; Neises, T.; Turchi, C. Optimal feed flow sequence for multi-effect distillation system integrated with supercritical carbon dioxide Brayton cycle for seawater desalination. *J. Clean Prod.* **2018**, *196*, 889–901. [CrossRef]
56. Sharan, P.; Neises, T.; Turchi, C. Thermal desalination via supercritical CO_2 Brayton cycle: Optimal system design and techno-economic analysis without reduction in cycle efficiency. *Appl. Therm. Eng.* **2019**, *152*, 499–514. [CrossRef]
57. Sharan, P.; Neises, T.; McTigue, J.D.; Turchi, C. Cogeneration using multi-effect distillation and a solar-powered supercritical carbon dioxide Brayton cycle. *Desalination* **2019**, *459*, 20–33. [CrossRef]
58. Cocco, D.; Serra, F. Performance Comparison of Two-Tank Direct and Thermocline Thermal Energy Storage Systems for 1MWe Class Concentrating Solar Power Plants. *Energy* **2015**, *81*, 526–536. [CrossRef]
59. Sánchez, D.; Frej, H.; Martínez, G.S.; Rodríguez, J.M.; Bennouna, E.G. Analysis of Thermal Energy Storage Solutions for a 1 MW CSP-ORC Power Plant. In Proceedings of the 3rd International Seminar on ORC Power Systems, Brussels, Belgium, 12–14 October 2015; pp. 1–10.

60. Rodríguez, J.M.; Sánchez, D.; Martínez, G.S.; Bennouna, E.G.; Ikken, B. Techno Economic Assessment of Thermal Energy Storage Solutions for a 1 MWe CSP-ORC Power Plant. *Sol. Energy* **2016**, *140*, 206–218. [CrossRef]
61. Petrollese, M.; Cau, G.; Cocco, D. The Ottana Solar Facility: Dispatchable Power from Small-Scale CSP Plants Based on ORC Systems. *Renew. Energy* **2020**, *147*, 2932–2943. [CrossRef]
62. Cascetta, M.; Petrollese, M.; Oyekale, J.; Cau, G. Thermocline vs. Two-Tank Direct Thermal Storage System for Concentrating Solar Power Plants: A Comparative Techno-Economic Assessment. *Int. J. Energy Res.* **2021**, *45*, 17721–17737. [CrossRef]
63. INMIS Energy S.A. Available online: http://www.inmis-energy.com/about-us/1-1-inmis (accessed on 29 December 2021).
64. Bell, I.H.; Wronski, J.; Quoilin, S.; Lemort, V. Pure and Pseudo-Pure Fluid Thermophysical Property Evaluation and the Open-Source Thermophysical Property Library Coolprop. *Ind. Eng. Chem. Res.* **2014**, *53*, 2498–2508. [CrossRef]
65. CoolProp. Available online: http://www.coolprop.org/ (accessed on 29 December 2021).
66. Bellos, E.; Sarakatsanis, I.; Tzivanidis, C. Investigation of Different Storage Systems for Solar-Driven Organic Rankine Cycle. *Appl. Syst. Innov.* **2020**, *3*, 52. [CrossRef]
67. Petrollese, M.; Arena, S.; Cascetta, M.; Casti, E.; Cau, G. Techno-Economic Comparison of Different Thermal Energy Storage Technologies for Medium-Scale CSP Plants. *AIP Conf. Proc.* **2019**, *2191*, 020128. [CrossRef]
68. Morin, G.; Dersch, J.; Platzer, W.; Eck, M.; Häberle, A. Comparison of Linear Fresnel and Parabolic Trough Collector Power Plants. *Sol. Energy* **2012**, *86*, 1–12. [CrossRef]
69. STAGE-STE. Medium Temperature Solar Collectors Database. Available online: http://stage-ste.psa.es/keydocuments/solarthermalcollectors.php (accessed on 29 December 2021).